J. Phys. Chem. A **1997,** *101,* 4142−4148

Geometric Structure and Second-Order Nonlinear Optical Response of Substituted Calix[4]arene Molecules: A Theoretical Study

E. Brouyère,[†] A. Persoons,[‡] and J. L. Brédas*,[†]

Centre de Recherche en Electronique et Photonique Moléculaires, Service de Chimie des Matériaux Nouveaux, Université de Mons-Hainaut, Place du Parc 20, B-7000 Mons, Belgium, and Center for Research on Molecular Electronics and Photonics, Laboratory of Chemical and Biological Dynamics, University of Leuven, Celestijnenlaan 200D, B-3001 Heverlee, Belgium

Received: March 12, 1997[⊗]

The geometries and second-order nonlinear optical properties of the four conformers of donor−acceptor-substituted calix[4]arene molecules are investigated by means of semiempirical quantum-chemical techniques. The evolution of the second-order polarizability β is analyzed with respect to changes in conformation and the theoretical results are compared with electric-field-induced second-harmonic generation and hyper-Rayleigh scattering experimental data. We point out the presence of strong $\pi-\pi$ cofacial interactions that shift the charge-transfer bands to shorter wavelengths; we rationalize the origin of the blue shift by studying the characteristics of a dimer.

I. Introduction

Owing to the interest devoted to photonic and optoelectronic devices, numerous experimental and theoretical investigations have aimed at characterizing the second-order nonlinear optical response of organic materials with large π-electron systems and asymmetric charge distributions.[1,2] Many studies have focused on push−pull conjugated molecules whose typical structure is characterized by a single conjugated backbone capped at each extremity by one (or more) donor and acceptor groups. Among prototypical compounds, we cite paranitroaniline,[3,4] various substituted stilbenes,[5−7] or polyene derivatives.[8,9] Extension of the conjugated pathway usually leads to an increase in the molecular hyperpolarizability β but is usually related to a shift of the charge-transfer absorption band to longer wavelengths (red shift), thus restricting the transparency window and the applicability of these materials for frequency doubling of laser light.

In this work, we investigate theoretically the second-order nonlinear optical properties of a new class of compounds: the calix[4]arenes[10,11] that present the peculiarity of containing four (donor−π-conjugated segment−acceptor) {D−π−A} units in a single molecule.[12] Their molecular structure consists in four functionalized phenol or anisole rings linked together by methylene bridges. Depending on the relative orientations of each phenol-like D−π−A unit, four calix[4]arene conformers can be distinguished, as sketched in Figure 1: (a) the cone conformer, displaying all the phenolic oxygens on the same side of the molecule in a calix-like shape; (b) the partial-cone (or so-called paco) conformer in which one of the D−π−A units is reversed with respect to the others; and (c) the 1,2 alternate (1,2-alt) and (d) 1,3 alternate (1,3-alt) conformations where two neighboring rings or two face-to-face phenol segments are reversed, respectively.

Our main goal is to evaluate the influence of changes in the relative orientations of the D−π−A units on the second-order nonlinear optical response of the calix[4]arene compounds. In section II, we briefly describe our methodology. Section III is devoted to an investigation of the geometric parameters of each calix[4]arene conformer, while section IV addresses the second-order nonlinear optical response.

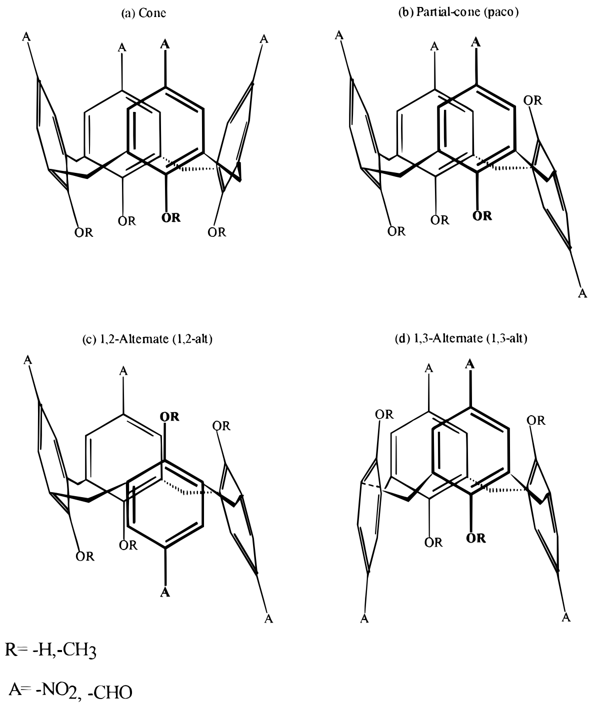

Figure 1. Schematic representation of the four conformers of the calix[4]arene molecule investigated in this work.

II. Methodology

The calix[4]arene compounds we consider contain nitro substituents on the upper rim and hydroxy or methoxy substituents on the lower rim. Because of the large size of these calix[4]arene systems, we have optimized the molecular structure of the four conformers at the semiempirical Hartree−Fock Austin Model 1 (AM1) level.[13] This method is known to provide reliable molecular geometry estimates for organic conjugated compounds.

We calculate the static components of the second-order molecular polarizability β in two ways. First, still using the

---

[†] Université de Mons-Hainaut.

[‡] University of Leuven.

[⊗] Abstract published in *Advance ACS Abstracts,* April 15, 1997.

S1089-5639(97)00931-6 CCC: $14.00

AM1 Hamiltonian, we consider the finite-field approach[14] in which the β components are obtained numerically by taking the derivative of the molecular dipole moment μ_i with respect to the electric field components F_j:

$$\mu_i = \mu_i^0 + \alpha_{ij}F_j + \frac{1}{2!}\beta_{ijk}F_jF_k + \frac{1}{3!}\gamma_{ijkl}F_jF_kF_l + ... \quad (1)$$

$$\beta_{ijk} = \frac{\partial^2\mu_i}{\partial F_j \partial F_k} \quad (2)$$

Here, μ_i^0 represents the permanent dipole moment; α_{ij}, β_{ijk}, and γ_{ijkl} are the tensor elements of the first-, second-, and third-order polarizabilities, respectively; F_j is the electric field component in the j direction; i, j, k, and l refer to the Cartesian axes.

In the second approach, we use the sum-over-states (SOS) perturbation technique[15] to estimate the molecular optical nonlinearities. Calculations are then performed at the intermediate neglect of differential overlap (INDO)[16]/single configuration interaction (SCI)[17] level on the basis of the AM1 geometries. This treatment leads to the transition energies and moments, as well as state dipole moments, which are to be plugged into the SOS β expression:

$$\beta_{ijk} = \sum_{\substack{\text{perm}\\ i,j,k}} \sum_{n,m\neq 0} \frac{\langle\psi_0|\mu_i|\psi_n\rangle\langle\psi_n|\mu_j|\psi_m\rangle\langle\psi_m|\mu_k|\psi_0\rangle}{(E_0 - E_n)(E_0 - E_m)} - \sum_{\substack{\text{perm}\\ i,j,k}} \langle\psi_0|\mu_j|\psi_0\rangle \sum_{n\neq 0} \frac{\langle\psi_0|\mu_i|\psi_n\rangle\langle\psi_n|\mu_k|\psi_0\rangle}{(E_0 - E_n)^2} \quad (3)$$

where $\langle\Psi_n|\mu_i|\Psi_m\rangle$ represents the electronic transition moment between the n and m states described by the wave functions Ψ_n and Ψ_m, respectively. Ψ_0 is the ground state; E_0 is the ground-state total energy, while E_n corresponds to the energy of excited state n.

Within the SCI formalism, the Coulomb repulsion integrals are expressed via the Mataga–Nishimoto[18] parameterization. The CI expansion is built with singlet excited state wavefunctions on the basis of 122 configurations obtained by the promotion of one electron from the highest 11 occupied molecular orbitals to the lowest 11 unoccupied levels. This number of configurations constitutes the minimal basis that should be used in the study of the calix[4]arene properties; indeed, the consideration of additional configuration does not result in any significant change in the transition moment and transition energy values.

This SOS technique also allows us to have access to the dynamic nonlinear optical properties. The β_{ijk} second-harmonic generation (SHG) terms are then calculated via a new expression for the denominator of eq 3 which becomes

$$(E_0 - E_n - 2\hbar\omega - i\Gamma_{0n})(E_0 - E_m - \hbar\omega - i\Gamma_{0m}) \quad (4)$$

In this expression, ω represents the frequency of the perturbating radiation field and Γ_{0n} is the damping factor associated to excited state n (here taken as equal to 0.1 eV).

To allow for a better comparison to the hyper-Rayleigh scattering (HRS)[19,20] and electric field-induced second harmonic generation (EFISHG)[21] experimental data, we have taken into account the respective appropriate expressions for β: (i) the β_{HRS} value is calculated from the following formula:

$$\beta_{\text{HRS}} = \sqrt{35/6\langle\beta^2_{\text{HRS}}\rangle} \quad (5)$$

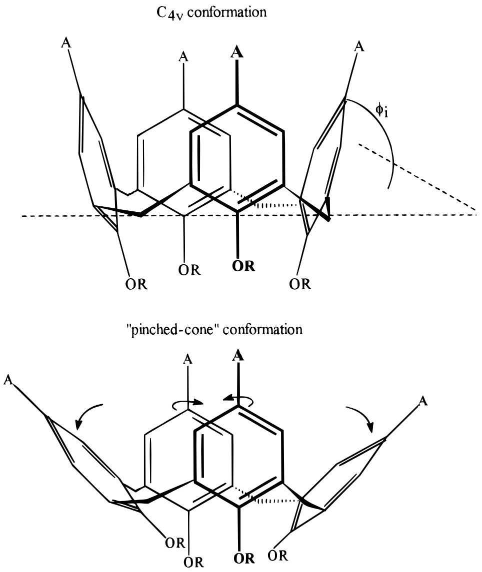

Figure 2. Sketch of the two optimized molecular structures of the cone conformer and representation of the ϕ_i dihedral angles between the plane of a phenyl ring and the mean plane of the four methylene groups.

where $\langle\beta^2_{\text{HRS}}\rangle$ is defined as[22]

$$\langle\beta^2_{\text{HRS}}\rangle = 6/35\sum_i \beta^2_{iii} + 16/105\sum_{i\neq j}\beta_{iii}\beta_{ijj} + 38/105\sum_{i\neq j}\beta^2_{ijj} + 16/105\sum_{ijk,\text{cycl.}}\beta_{iij}\beta_{jkk} + 20/35\beta^2_{ijk} \quad i,j,k = x,y,z \quad (6)$$

and (ii) β_{EFISHG} is expressed as[23]

$$\beta_{\text{EFISHG}} = \beta_{zzz} + 1/3(\beta_{zxx} + \beta_{zyy} + \beta_{xzx} + \beta_{yzy} + \beta_{xxz} + \beta_{yyz}) \quad (7)$$

where the permanent dipole moment is aligned along the z direction.

III. Geometric Structure of the Calix[4]arene Conformers

We characterize the geometries of the calix[4]arene molecules by the ϕ_i dihedral angles between the plane of each phenylene ring and the mean plane of the four methylene groups, see Figure 2. We report in Table 1a the AM1-optimized dihedral angles for each conformer of the calix[4]arenes; in order to establish an easy comparison, we present in Table 1b experimental X-ray and/or theoretical molecular mechanics (MM) data collected from the literature.[24-26]

The cone conformer is known for its multiple applications in the field of supramolecular "host–guest" chemistry where its cone-shaped framework allows for an easy complexation of numerous chemical species such as cations, anions, or small neutral molecules.[27-33] The cone appears in two possible molecular arrangements: (i) a structure with C_{4v} symmetry where the four D–π–A units present similar dihedral angles with respect to the mean plane of the four methylene groups; and (ii) an approximate C_{2v} conformation, usually referred to as the "pinched-cone" conformer,[34] which displays two parallel cofacial chromophores while the other two phenolic entities flatten, see Figure 2 (note that flattening refers to a decrease in dihedral angle ϕ_i). The results of the AM1 calculations indicate that the C_{2v} conformer is thermodynamically much more stable than the C_{4v} geometry by some 120 kcal/mol. This difference results from the large distortion observed at the level of the CH_2–ϕ–CH_2 valence angles for the C_{4v} conformation (101.5°),

TABLE 1: Presentation of (a) AM1 and (b) Molecular Mechanics (MM) and Experimental (X-ray) Dihedral Angles (in Degrees)[a]

conformation	lower rim substituent	upper rim substituent	method	ϕ_1	ϕ_2	ϕ_3	ϕ_4	refs
			(a) AM1 Dihedral Angles					
cone C_4v	4$-$OH	4$-$NO$_2$	AM1	62	62	62	62	this work
cone C_4v	4$-$OCH$_3$	4$-$NO$_2$	AM1	66	66	66	66	this work
pinched-cone	4$-$OH	4$-$NO$_2$	AM1	73	34	75	32	this work
pinched-cone	4$-$OCH$_3$	4$-$NO$_2$	AM1	76	38	78	33	this work
paco	4$-$OH	4$-$NO$_2$	AM1	75.5	−76	73.5	40	this work
paco	4$-$OCH$_3$	4$-$NO$_2$	AM1	78.5	−78	79.5	32	this work
1,2-alt	4$-$OH	4$-$NO$_2$	AM1	86	−74	−71	26	this work
1,2-alt	4$-$OCH$_3$	4$-$NO$_2$	AM1	70	−66	−64	64	this work
1,3-alt	4$-$OH	4$-$NO$_2$	AM1	79	−76	78	−79	this work
1,3-alt	4$-$OCH$_3$	4$-$NO$_2$	AM1	80	−81	78	−89	this work
			(b) Molecular Mechanics and Experimental Dihedral Angles					
cone C_4v	4$-$OH	4-*tert*-octyl	X-ray (MM2)	57 (58.1)	57 (58.1)	57 (58.1)	57 (58.1)	24
pinched-cone	2$-$OH, 2$-$OCH$_3$	4-*tert*-octyl	X-ray (MM2)	82.7 (80.4)	38.4 (38.4)	82.2 (80.4)	34.4 (38.4)	24
pinched-cone	2$-$OH, 2$-$OCH$_3$	4$-$H	X-ray (MM2)	75.5 (77.6)	43.9 (37.5)	78.3 (77.6)	37.0 (37.5)	24
pinched-cone	4$-$OCH$_3$	4-*tert*-butyl	MM3	83.1	44.5	83.1	44.5	26
paco	4$-$OCH$_3$	4-*tert*-butyl	X-ray (MM2)	88.3 (88.3)	-88.0 (−88.9)	84.8 (89.9)	35.3 (25.2)	24
paco	4$-$OCH$_3$	4-*tert*-butyl	MM3	89.2	−91.8	88.7	34.1	26
paco	4$-$OCH$_2$CH$_3$	4-*tert*-butyl	X-ray	92.0	−96.6	87.2	41.7	25
1,2-alt	4$-$OCH$_3$	4-*tert*-butyl	MM3	63.8	−63.7	-63.7	63.8	26
1,2-alt	4$-$OCH$_2$CH$_3$	4-*tert*-butyl	X-ray	83.8	−80.8	−47.5	47.8	25
1,3-alt	4$-$OCH$_3$	4-*tert*-butyl	MM3	87.8	−87.9	88.0	−87.9	26

[a] Dihedral angles are between the plane of the phenylene rings and the mean plane of the four methylene groups for the four conformations of nitrocalix[4]arenes with $-$OH or $-$OCH$_3$ substituents at the lower rim.

a while the pinched-cone conformer is found to present CH$_2$$-$$\phi$$-CH_2$ angles of 110.9°, a very close to the 109.47° ideal value for sp^3-hybridized carbons and in very good agreement with the X-ray-averaged CH$_2$$-$$\phi$$-CH_2$ bond angle value of 111.50° reported by Lipkowitz *et al.*[35] We point out that the replacement of hydroxy groups by methoxy groups causes a slight "upright" of the chromophoric units, which is attributed to the loss of Hydrogen bonds at the lower rim of the molecule as well, so as to increase the substituent size at this level.

Our calculations are consistent with the X-ray data, especially in providing an asymmetric pinched-cone geometry, while MM calculations suggest a perfect C_{2v} conformation. We also note that the AM1 method underestimates the ϕ_i dihedral angles except for the cone C_{4v} conformation; however, the X-ray experimental geometry refers to a situation in which the C_{4v} cone complexes a toluene molecule. The introduction of the organic molecule into the cavity of the calix[4]arene compound is expected to lead to some flattening of the phenolic rings, giving rise to a decrease in ϕ_i angles.

The paco conformer has been less extensively described than the cone conformer; it displays a three-dimensional structure in which a D$-$$\pi$$-$A segment assumes a reversed orientation; this introduces a negative ϕ_i dihedral angle in the description of the molecule. We note a good correspondence between the AM1 and X-ray geometries, despite the underestimation of the ϕ_i angles for the nonflattened rings.

The 1,2-alt conformer contains two neighboring reversed phenol units and, when the donor substituents are methoxy groups, nearly displays C$_i$ symmetry in very good agreement with the MM geometry calculated by Shinkai *et al.*[26] When $-$OH groups are used as donors, we observe that one of the rings rotates in order to come nearly into the plane of the four methylenes; this allows to maximize the strength of the H-bonds, as sketched in Figure 3. If we compare our theoretical geometries with the X-ray molecular structure presented in Table 1b, we note a large difference in the ϕ_i dihedral angle values. We attribute this discrepancy to the fact that the X-ray data are relative to the single-crystal structure of the tetraethylether of *p*-*tert*-butylcalix[4]arene interacting with two molecules of dichloromethane and loosing, in this way, a symmetric structure in the solid state. In solution, the structure is rocking due to its flexibility and can recover an averaged symmetrical geometry.

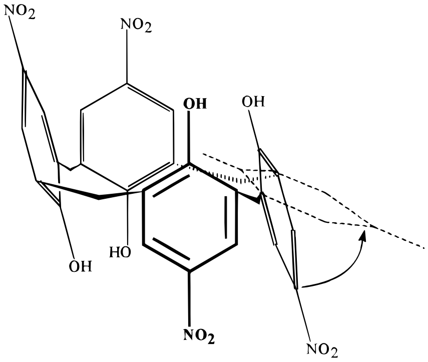

Figure 3. Illustration of the rotation of a chromophoric unit occurring in the 1,2-alt conformer upon $-$OH substitution.

TABLE 2: AM1 Relative Stabilities (in kcal/mol) for the Four Conformers of Nitrocalix[4]arene Molecules

		conformations			
	donor groups	pinched-cone	paco	1,2-alt	1,3-alt
$\Delta H°$	4-OH	0.0	5.6	6.4	9.8
	4-OCH$_3$	0.0	−1.1	0.2	−0.6

Finally, the 1,3-alt conformer shows two pairs of cofacial chromophores pointing in opposite directions with similar ϕ_i dihedral angles. The introduction of methoxy groups at the lower rim of the molecule induces a slight increase of these angles, as already observed in the other calix[4]arene conformers.

In addition to the change in geometry, the modulation of the nature of the donor substituents disturbs the relative stabilities between the four calix conformers, as illustrated in Table 2. Upon $-$OH functionalization,[36] the stability order is mainly controlled by the number of H-bonds at the lower rim of the molecule. As expected, the most stable geometry corresponds to the pinched-cone conformer that presents four H-bonds in

TABLE 3: Theoretical and Experimental Dipole Moment μ (in D), Second-Order Polarizability β (in 10^{-30} esu), and Absorption Maximum λ_{max} (in nm) for the Calix[4]arenes under Different Substitution Pathways, as Well as for Monomers and Dimers of *o,o′*-Dimethyl-*p*-nitrophenol, *o,o′*-Dimethyl-*p*-nitroanisol, and *o,o′*-Dimethyl-*p*-hydroxybenzaldehyde

			AM1-FF			INDO-SCI-SOS				experl results			
conformation	donor	acceptor	μ	β_{EFISHG}	β_{HRS}	μ	β_{EFISHG}	β_{HRS}	λ_{max}	μ	β_{EFISHG}[a]	β_{HRS}[a]	λ_{max}
p-cone	4−OH	4−NO_2	14.5	5.4	5.4	17.2	22.9	23.8	290				
paco			8.0	1.8	1.8	9.6	12.5	12.8	290				
1,2-alt			3.9	2.3	2.6	4.5	6.3	7.1	290				
1,3-alt			0.1	0.0	0.0	0.1	0.1	0.3	290				
p-cone	4−OCH_3	4−NO_2	18.1	2.1	2.2	21.5	22.1	24.4	290	13.8	30.0	27.0	291
paco			9.4	0.7	0.8	11.2	11.8	13.8	290	6.7	27.0		291
1,2-alt			0.3	0.1	0.1	0.3	1.0	1.1	290				
1,3-alt			0.0	0.0	0.0	0.4	0.8	0.8	290	0.0	0.0	0.0	291
p-cone	4−OCH_3	4−CHO	6.3	11.4	11.4	10.2	17.4	18.5	263	10.7	19.0		269
paco			3.5	5.0	5.1	5.7	5.9	8.2	261				
1,2-alt			1.5	3.7	4.1	2.4	0.5	0.6	262				
1,3-alt			0.0	0.0	0.1	0.0	0.2	0.6	261				
monomer	−OH	−NO_2	5.6	4.6	4.6	6.6	12.5	13.1	301	4.6	12.0		302
dimer			15.5	7.9	8.0	12.6	18.3	18.3	284				
monomer	−OCH_3	−NO_2	5.9	5.4	5.4	6.3	11.5	13.3	295	5.0	12.0		288
dimer			11.4	7.3	7.4	12.2	18.9	19.9	277				
monomer	-OCH_3	-CHO	3.5	1.4	1.4	3.9	6.6	8.7	272	3.2	8.0		269[b]
dimer			6.7	3.0	3.0	7.6	14.5	15.8	256				

[a] Experimental EFISHG[12,38] and HRS[37,39] β's concern tetrapropoxynitrocalix[4]arenes and are measured at a fundamental wavelength of 1064 nm. [b] Experiment relates the behaviour of *p*-hydroxybenzaldehyde.

its structure. The paco conformer is found to be the second most stable structure, since it displays two neighboring H-bonds that allow for a better charge delocalization than the 1,2-alt compound containing two separate and localized H-bonds. Due to the lack of H-bond, the 1,3-alt conformer is the highest energy molecular system. The introduction of methoxy groups as donors leads to a modification in the relative stabilities of the calix[4]arene conformers. The loss of H-bonds and the steric hindrance resulting from the presence of more bulky groups at the lower rim give in decreasing order: paco > 1,3-alt > cone > 1,2-alt.

We have also considered the substitution of the nitro groups by formyl groups to form formylcalix[4]arenes; the latter do not show modifications in the ϕ_i dihedral angles with respect to the nitro-substituted compounds. This stresses that such a change in acceptor entities does not significantly affect the molecular geometry of the calix[4]arene conformers.

IV. Nonlinear Optical Response

We report in Table 3 the dipole moments, second-order polarizabilities, and λ_{max} obtained both experimentally and theoretically for each calix[4]arene conformer with different substitution pathways; note that the results reported for the cone conformation correspond to the pinched-cone conformer. We emphasize the overall good agreement of the SOS results in comparison to the experimental data, as well as the significant underestimation of the hyperpolarizability values provided by the AM1/finite-field analysis. In our opinion, the inadequacy of the AM1/finite-field technique originates in the lack of inclusion of correlation effects; these are expected to play a major role in the description of the second-order nonlinear response in calix[4]arene compounds that present interacting subunits.

We also note a discrepancy between theoretical and experimental β estimates for the paco conformation; the theory predicts a paco β value more or less equal to half that of the cone value, while the EFISHG measurements performed at the wavelength of 1064 nm (1.16 eV) lead to a paco β value close to that of the cone conformer. Recently, new HRS measurements[37] have contradicted the EFISHG evaluations; the HRS β values for the cone and paco conformers, measured at the fundamental wavelength of 900 nm (1.37 eV), are 36 × 10^{-30} esu for the cone conformer and 19 × 10^{-30} esu for paco. These HRS data and their ratio are in excellent agreement with the SOS theoretical description of the NLO properties of the two conformers. The EFISHG response of the paco conformer should thus be treated with much caution. We stress that, at the fundamental wavelengths of 1064 and 900 nm, there are no significant resonance effects that lead to a strong enhancement of the second-order polarizability; this is illustrated in Figure 4.

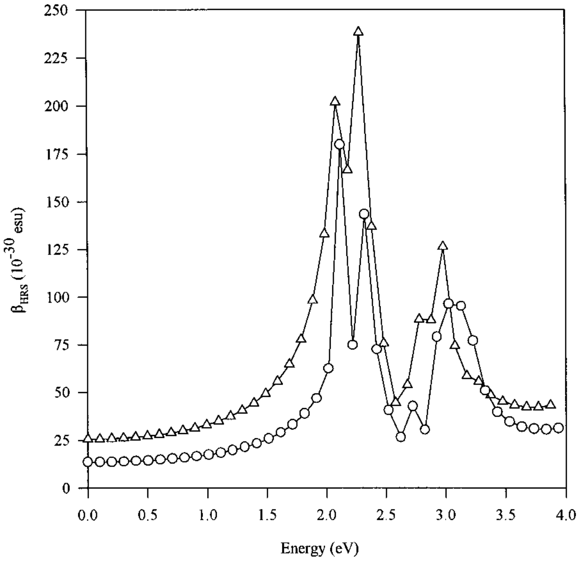

Figure 4. Theoretical INDO/SCI-sum-over-states frequency dispersion of the second-harmonic generation (SHG) spectra for the cone (△) and paco (○) conformers. The abscissa corresponds to the energy of the fundamental beam.

The theoretical evolution of the second-order nonlinear optical polarizabilities can be related to the changes occurring in the conformation of the calix[4]arenes. The β values follow the decreasing sequence: cone > paco > 1,2-alt > 1,3-alt; this ordering can be rationalized by an analysis of the total charge transfer (CT) within the calix[4]arene compound that is illustrated in Figure 5. The nitrocalix[4]arenes possess two main low-lying CT excited states located at 4.3 and 4.5 eV, respectively. In the pinched-cone conformation, there exist four

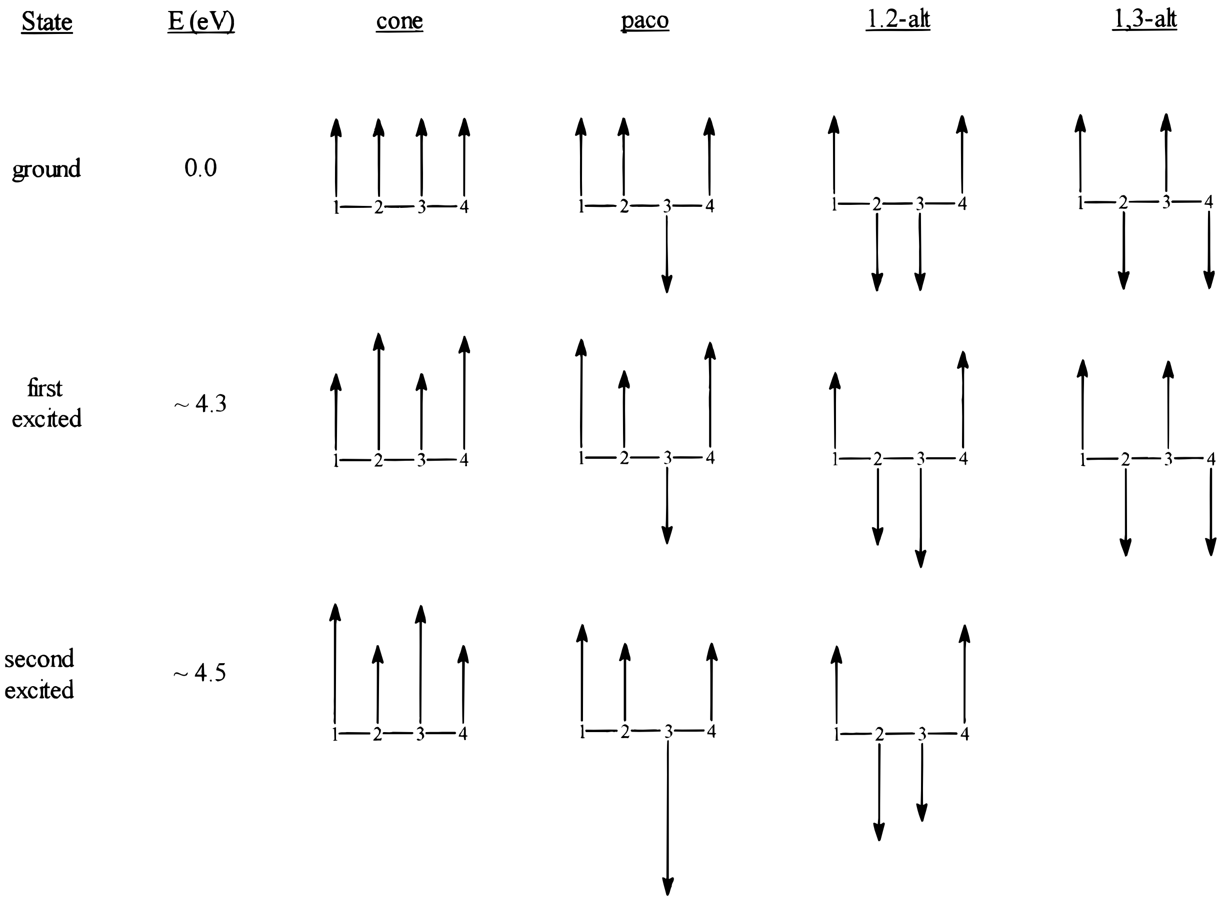

Figure 5. Sketch of the charge transfer intensity in each D$-\pi-$A unit of the four calix[4]arene conformers. The numbers 1, 2, 3, 4 represent the disubstituted phenylene rings in the calix molecule, and the arrows describe the intensity and direction of the charge transfer within these units.

codirectional contributions to the global charge tranfer that have the same intensities in the ground state which evolve to a situation presenting two face-to-face dominant CT excitations in the two excited states, see Figure 5. As these components evolve in the same direction, we obtain a global enhancement of CT within the calix[4]arene compound in the excited state leading to a rather large β value. The second CT excited state of the paco conformer displays, as expected, a large opposite contribution due to the presence of the reversed ring in the molecule; the β value is therefore smaller than that in the pinched-cone conformer.

For the 1,2-alt conformer, there occurs a further decrease in β value, the appearance of a second inverted ring in the calix[4]arene structure inducing a second opposite CT component. The β decrease is more significant when the donors are methoxy groups instead of hydroxy substituents. The second-order polarizability of the $-OCH_3$-substituted 1,2-alt conformer is vanishingly small due to the near C_i symmetry of the molecule, the $-$OH-substituted molecule displays a ring that nearly lies in the same plane as that of the methylene groups (see Figure 3), and this feature introduces a weaker cancelation between the D$-\pi-$A units pointing in different directions and leads overall to a somewhat higher β value. The 1,3-alt form shows a structure with two pairs of cofacial rings pointing in opposite directions and presenting the same CT intensities; this leads to a total cancelation of the vector part of the second-order nonlinear optical response β. These evolutions reflect the strong connection between the molecular conformation and the nonlinear optical properties of the molecule.

The replacement of the $-NO_2$ acceptor groups by formyl ($-$CHO) groups results in a decrease in the theoretical values of μ and β, in agreement with experiment.[12] We observe the same trends for the CT evolution upon excitation when considering the various calix conformers; however, we note a decrease in CT amplitude within each D$-\pi-$A chromophoric unit that reflects the weaker acceptor strength of the formyl groups. Also, there occurs a slight increase in the low-lying CT excited-state energies; since these energies appear in the denominator of the SOS expression, this also contributes to reducing the β values.

We now turn to a discussion of the NLO response of the cone conformer, in the case of nitro and hydroxy substitutions. The μ and β values are reasonably large, which justifies the incorporation of cone calix[4]arenes as nonlinear optical chromophores in poled polymers.[39] However, we note that, despite the fact that four D$-\pi-$A chromophores are pointing in the same direction, the β response (23.8×10^{-30} esu) is significantly lower than 4 times the β response of an *o*,*o*′-dimethyl-*p*-nitrophenol unit ($(4 \times 13.2=52.4) \times 10^{-30}$ esu). To quantify the origin of this lower β value for the cone calixarene, we first evaluate the nonlinear optical behavior of the pinched-cone conformer in a vectorial way. As the D$-\pi-$A units constituting the calix[4]arene compound are not perfectly vertical, their contributions to the molecular β response are weighted by the sine of the ϕ_i dihedral angle between the plane of the phenylene ring and the plane defined by the four methylene groups. This simple vectorial analysis would lead to a pinched-cone β value of about 39.4×10^{-30} esu that is lower than 4 times the β value of a single D$-\pi-$A unit but still higher than both the experimental and calculated second-order nonlinear responses for the calix[4]arene in the cone conformation.

Thus, an additional effect needs to be considered to rationalize the β value. In this context, it is useful to refer to the studies of Di Bella *et al.*[40] who have described the β evolution of a

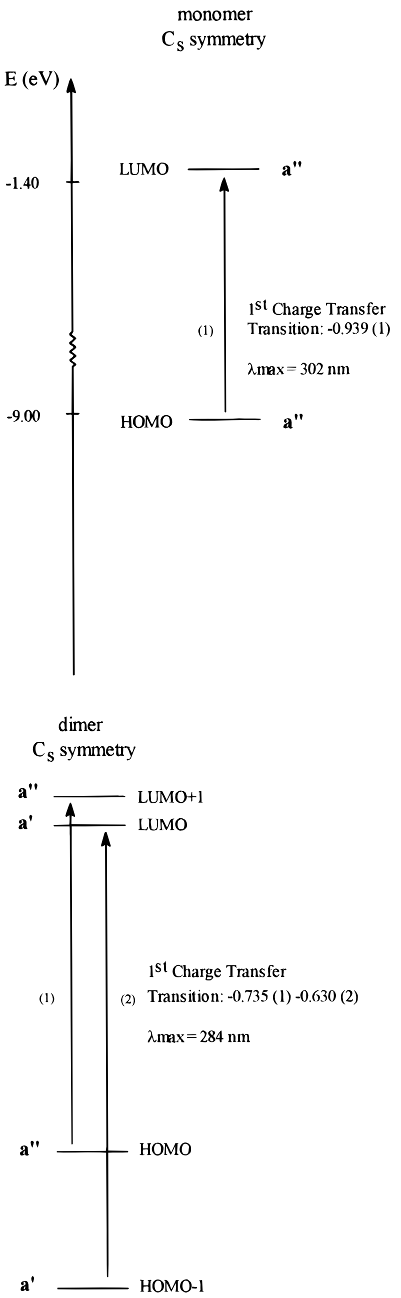

Figure 6. Illustration of the one-electron transition(s) describing the first charge transfer excited state of an *o,o′*-dimethyl-*p*-nitrophenol molecule and of the corresponding dimer.

dimer built from cofacial *p*-nitroaniline (pNA) molecules, as a function of the distance *R* between the planes of the two rings. In comparison to the ideal β value that would be equal to twice the β pNA value, these authors find that the second-order nonlinear polarizability of the dimer decreases for distances *R* in the range 3.5−9.0 Å, this behavior being related to interactions between the two molecular π systems.[40]

In the calix[4]arenes, the cofacial chromophores are calculated to be separated by 4.5 Å (in good agreement with the experimental observations[12]) and are thus in the range of the “destructive” $\pi-\pi$ interactions shown by Di Bella *et al.*[40] To better apprehend this effect, we have compared the electronic and optical properties of the *o,o′*-dimethyl-*p*-nitrophenol molecule and the corresponding dimer with a distance between the planes of the phenylene rings frozen at 4.5 Å; these calculations are performed at the INDO/SCI level.

The first CT transition of the *o,o′*-dimethyl-*p*-nitrophenol is calculated at 301 nm, in excellent agreement with the 302 nm experimental value[12], and is mainly characterized by the promotion of an electron from the HOMO (highest occupied molecular orbital) level to the LUMO (lowest unoccupied molecular orbitals) level. In the dimer, both the HOMO and LUMO levels split. The LUMO orbital of the complex adopts an a′ symmetry giving rise to a [HOMO a″ → LUMO a′] transition which is polarized along the stacking axis of the dimer. As a consequence of the difficulty of intermolecular charge transfer at such large intermolecular distances, the dipolar electronic transition moment along this axis is vanishing and the HOMO → LUMO transition probability goes to zero. Actually, in the dimer, the first CT excited state corresponds to a strong mixing of two electronic transitions, see Figure 6, which involves a one-electron promotion from HOMO to LUMO + 1 and from HOMO − 1 to LUMO. These transitions, occurring along the molecular axes, rationalize the blue shift of the low-lying CT band of the dimer since they involve more energetic transitions than in the monomer case. As a consequence, the dimer presents a β value which is around 18×10^{-30} esu, lower than twice that of the response of an isolated molecule (26.2×10^{-30} esu). We stress that the same behavior is obtained for the other two substitution patterns, *i.e.*, in the case of *o,o′*-dimethyl-*p*-nitroanisol and *o,o′*-dimethyl-*p*-hydroxybenzaldehyde monomers and dimers. Cofacial interactions are thus confirmed to constitute a second factor that is responsible for decreasing the β value of the calix[4]arene cone conformer.

V. Synopsis

In this work, we have theoretically analyzed the geometry and second-order nonlinear optical properties of supramolecules displaying more than a single D−π−A unit within their molecular structures: the calix[4]arenes. The connection between the geometric structure and optical properties of the systems has been illustrated by evaluating the NLO response of each calix[4]arene conformer at the correlated level. We were able to quantify the impact on the β values of the strong $\pi-\pi$ interactions that take place between cofacial D−π−A units and lead to a blue shift in the low-lying charge transfer band.

Acknowledgment. This work is partly supported by the Belgian Prime Minister Office of Science Policy (SSTC) “Pôle d’Attraction Interuniversitaire en Chimie Supramoléculaire et Catalyse” (Grant PAI 4/11), FNRS/FRFC, and an IBM Academic Joint Study. We thank Dr. E. Hendrickx for a critical reading of the manuscript.

References and Notes

(1) Chemla, D. S.; Zyss, J. *Nonlinear Optical Properties of Organic Molecules and Crystals*; Academic Press, Inc.; New York, 1987.

(2) Prasad, P. N.; Williams, D. J. *Introduction to Nonlinear Opticals Effects in Molecules and Polymers*; Wiley Interscience: New York, 1991.

(3) Levine, B. F. *Chem. Phys. Lett.* **1976**, *37*, 516

(4) Sim, F.; Chin, S.; Dupuis, M.; Rice, J. E. *J. Am. Chem. Soc.* **1993**, *115*, 1158.

(5) Marder S. R.; Beretan, D. N., Cheng, L.-T. *Science* **1991**, *252*, 103.

(6) Cheng, L.-T.; Tam, W.; Stevenson, S. H.; Meredith, G. R.; Rikken, G.; Marder S. R. *J. Phys. Chem.* **1991**, *95*, 10631. Cheng, L.-T.; Tam, W.; Marder S. R.; Stiegman, A. E.; Rikken, G.; Spangler, C. W. *J. Phys. Chem.* **1991**, *95*, 10643.

(7) Meyers, F.; Brédas, J. L.; Zyss, J. *J. Am. Chem. Soc.* **1992**, *114*, 2914.

(8) Matsuzawa, N.; Dixon, D. A. *Int. S. Quantum. Chem.* **1992**, *44*, 497. Dehu, C.; Meyers, F.; Brédas, J. L. *J. Am. Chem. Soc.* **1993**, *115*, 6198. Blanchard-Desce, M.; Wortmann, R.; Lebus, S.; Lehn, J. M.; Krämer, P. *Chem. Phys. Lett.* **1995**, *243*, 526.

(9) Marder, S. R.; Gorman, C. B.; Meyers, F.; Perry, J. W.; Bourhill, G.; Brédas, J. L.; Pierce B. M. *Science* **1994**, *265*, 632.

(10) Gutsche, D. C. *Calixarenes*; The Royal Society of Chemistry: Cambridge, **1989**. Böhmer, V. *Angew. Chem., Int. Ed. Engl.* **1995**, *34*, 713.

(11) van Dienst, E.; Bakker, I. I. W.; Engbersen, J. F. J.; Verboom, W.; Reinhoudt, D. N. *Pure Appl. Chem.* **1993**, *65*, 387.

(12) Kelderman, E.; Derhaeg, L.; Heesink, G. J. T.; Verboom, W.; Engbersen, J. F. J.; van Hulst, N. F.; Persoons, A.; Reinhoudt, D. N. *Angew. Chem., Int. Ed. Engl.* **1992**, *31*, 1075. Kelderman, E.; Derhaeg, L.; Verboom, W.; Engbersen, J. F. J.; Harkema, S.; Persoons, A.; Reinhoudt, D. N. *Supramol. Chem.* **1993**, *2*, 183.

(13) Dewar, M. J. S.; Zoebisch, E. G.; Healy, E. F.; Stewart, J. J. P. *J. Am. Chem. Soc.* **1985**, *107*, 3902.

(14) Kurtz, H. A.; Stewart, J. J. P.; Dieter, K. M. *J. Comput. Chem.* **1990**, *11*, 82.

(15) Orr, B. J.; Ward, J. F. *Mol. Phys.* **1971**, *20*, 513.

(16) Pople, J. A.; Beveridge, D. L.; Dobosh, P. A. *J. Chem. Phys.* **1967**, *47*, 2026.

(17) Ridley, J. E.; Zerner, M. C. *Theor. Chim. Acta* **1973**, *32*, 111.

(18) Pierce, B. M. *J. Chem. Phys.* **1989**, *91*, 791.

(19) Clays, K.; Persoons, A. *Phys. Rev. Lett.* **1991**, *66*, 2980.

(20) Clays, K.; Persoons, A. *Rev. Sci. Instrum.* **1992**, *63*, 3285.

(21) Levine, B. F.; Bethea, C. G. *J. Chem. Phys.* **1975**, *63*, 2666.

(22) Cyvin, S. F.; Rauch, J. E.; Decius, J. C. *J. Chem. Phys.* **1965**, *43*, 4083.

(23) Lalama, S. J.; Garito A. F. *Phys. Rev. A* **1979**, *20*, 1179.

(24) Grootenhuis, P. D. J.; Kollman, P. A.; Groenen, L. C.; Reinhoudt, D. N.; van Hummel, G. J.; Ugozolli, F.; Andreetti, G. D. *J. Am. Chem. Soc.* **1990**, *112*, 4165.

(25) Groenen, L. C.; van Loon, J.-D.; Verboom, W.; Harkema, S.; Casnati, A.; Ungaro, R.; Pochini, A.; Ugozolli, F.; Reinhoudt, D. N. *J. Am. Chem. Soc.* **1991**, *113*, 2385.

(26) Harada, T.; Rudzinski, J. M.; Shinkai, S. *J. Chem. Soc., Perkin Trans. 2* **1992**, 2109.

(27) Böhmer, V.; O'Sullivan, P. *Trends Polym. Sci.* **1993**, *1*, 267.

(28) Ungaro, R.; Pochini, A. *Frontiers in Supramolecular Organic Chemistry and Photochemistry*; VCH: Weinheim, 1991; p. 57.

(29) Guilbaud, P.; Varnek, A.; Wipff, G. *J. Am. Chem. Soc.* **1993**, *115*, 8298.

(30) Miyamoto, S.; Kollman, P. A. *J. Am. Chem. Soc.* **1992**, *114*, 3668.

(31) Bakker, W. I. I.; Haas, M.; Khoo-Beattie, C.; Ostaszewski, R.; Franken, S. M.; den Hertog, H. J.; Verboom, W.; de Zeeuw, D.; Harkema, S.; Reinhoudt, D. N. *J. Am. Chem. Soc.* **1994**, *116*, 123.

(32) Ball, P. *Nature* **1994**, *371*, 202.

(33) Ogata, M.; Fujimoto, K.; Shinkai, S. *J. Am. Chem. Soc.* **1994**, *116*, 4505.

(34) Conner, M.; Janout, V.; Regen, S. L. *J. Am. Chem. Soc.* **1991**, *113*, 9670.

(35) Lipkowitz, K. B.; Pearl, G. *J. Org. Chem.* **1993**, *58*, 6729.

(36) Fisher, S.; Grootenhuis, P. D. J.; Groenen, L. C.; van Hoorn, W. P.; van Veggel, F. C. J. M.; Reinhoudt, D. N.; Karplus, M. *J. Am. Chem. Soc.* **1995**, *117*, 1611.

(37) Kenis, P. J. A. Private communication.

(38) Kelderman, E. Private communication.

(39) Kelderman, E.; Heesink, G. J. T.; Derhaeg, L.; Verbiest, T.; Klaase, P. T. A.; Verboom, W.; Engbersen, J. F. J.; van Hulst, N. F.; Clays, K.; Persoons, A.; Reinhoudt, D. N. *Adv. Mater.* **1993**, *5*, 925.

(40) Di Bella, S.; Ratner, M. A.; Marks, T. J. *J. Am. Chem. Soc.* **1992**, *114*, 5842.